Collective excitations in quantum wires formed in mesoporous silica

2002 J. Phys.: Condens. Matter 14 1915

(http://iopscience.iop.org/0953-8984/14/8/319)

INSTITUTE OF PHYSICS PUBLISHING JOURNAL OF PHYSICS: CONDENSED MATTER

J. Phys.: Condens. Matter **14** (2002) 1915–1921 PII: S0953-8984(02)28902-X

Collective excitations in quantum wires formed in mesoporous silica

S M Bose[1,3] **and P Longe**[2]

[1] Department of Physics, Drexel University, Philadelphia, PA 19104, USA
[2] Institut de Physique B5, Universite de Liege, Sart-Tilman, B-4000 Liege, Belgium

E-mail: bose@drexel.edu

Received 18 September 2001
Published 15 February 2002
Online at stacks.iop.org/JPhysCM/14/1915

Abstract

The collective electronic excitation (plasmon) modes of a three-dimensional distribution of quantum wires such as those produced in mesoporous silica (MCM-41) have been calculated. The plasmon frequencies are found to be strongly dispersive for momentum components both parallel and perpendicular to the axes of the quantum wires. The lowest subband plasmon modes are acoustic for momentum components parallel to the wires and they are optical for momentum components perpendicular to the wires. A comparison with the plasmon modes of a single quantum wire or of a uniform three-dimensional electron gas (3DEG) indicates that for plasmon wavelengths small (wavevector q large) compared with inter-quantum-wire distance a, i.e. for $aq \gg 1$, the calculated modes would tend to those of a single quantum wire, and they tend to those of the 3DEG for large wavelengths ($aq \ll 1$). The contribution of the lattice formed by the quantum wires in mesoporous silica is dominant for intermediate wavelengths ($0 \ll aq \ll \infty$).

1. Introduction

In recent years there has been a surge of interest in the production and characterization of microstructures such as quantum wells, quantum dots, quantum wires etc, because of their potential industrial applications. Techniques such as molecular beam epitaxy (MBE) and metallo-organic chemical vapour deposition (MOCVD), along with holographic patterning, reactive ion etching, anode thinning etc, are being used with great success to produce good-quality microstructures [1–7]. The reduced dimensionality of these structures introduces many interesting new physical properties to these systems, which are also being studied for their basic scientific interest [8–14]. While many studies have been carried out in a single quantum wire or a two-dimensional array of quantum wires, more recently three-dimensional superlattices (3DSLs) of quantum wires have been produced and their properties are being studied [15–17].

[3] Author to whom any correspondence should be addressed.

0953-8984/02/081915+07$30.00

Perhaps most interesting is the recent discovery by Mobil Oil Company of the mesosporic silica with nanoscopic pores distributed in lattices of hexagonal (MCM-41), cubic (MCM-48) and lamellar (MCM-50) symmetry [18, 19]. Several semiconducting compounds have now been implanted into MCM-41 to obtain regular arrays of quantum wires arranged in a hexagonal close-packed structure and their physical properties are being studied [20–26].

In this paper, we calculate the collective excitation (plasmon) modes of a 3DSL of quantum wires distributed in a hexagonal lattice similar to the quantum wires in MCM-41. We do this by using and extending a model previously developed by us for the study of a superlattice formed by a layered two-dimensional electron gas (2DEG) system [27]. Since in the low-energy and low-electron-density regime the electrons in the quantum wires are in the lowest subband, and for computational simplicity, in this paper we calculate the plasmon modes for the lowest subband only, even though the calculation can be extended to higher subbands in a straightforward way [13]. Taking into account both the intra- and inter-quantum-wire electronic Coulomb interaction we have carried out a calculation of the dielectric function of the quantum wires arranged in a hexagonal close-packed structure in the random phase approximation (RPA). We then obtain the collective excitation (plasmon) modes by imposing the condition of cancellation of the real part of the (complex) dielectric function, i.e. from

$$\operatorname{Re}\varepsilon(q,\omega_p)=0. \tag{1}$$

It should be mentioned that study of the electronic properties of a quasi-one-dimensional conductor has a long history and some of the pioneering work has been done in this area by Luttinger [28], Jerome and Schulz [29], Schulz [30] and others.

In section 2 we present the calculation of the plasmon frequencies for the 3DSL and compare them with the plasmon frequencies of a single quantum wire and those of a uniform 3DEG. In section 3, we present a brief discussion and conclusions of this paper.

2. Three-dimensional quantum wire superlattice

We consider a 3DSL of quantum wires consisting of parallel 1DEGs arranged in a hexagonal closed packed structure and separated by a distance a. A cross section perpendicular to the quantum wire axes appears as a close-packed triangular two-dimensional Bravais lattice with a as a lattice constant as shown in the lower right part of figure 1. This system is not formally different from the multilayered electron gas system treated in [27], and considerations similar to those of this reference yield

$$\operatorname{Re}\varepsilon(q,\omega_p)\equiv 1+2e^2F(q,\kappa)\Pi_1(q,\omega)=0 \tag{2}$$

where the geometric factor $F(q,\kappa)$ corresponding to the distribution of the quantum wires in a hexagonal lattice is given by

$$F(q,\kappa)=\sum_{n_1=-\infty}^{\infty}\sum_{n_2=-\infty}^{\infty}\mathrm{e}^{\mathrm{i}(\kappa_1 n_1+\kappa_2 n_2)}K_0(qa|n|) \tag{3}$$

where (n_1,n_2) and (κ_1,κ_2) are two-dimensional vectors defined in the direct lattice and in the reciprocal lattice, respectively, and K_0 is the modified Bessel function of the second kind. More precisely, in the direct lattice, one has

$$\boldsymbol{n}=(n_1\boldsymbol{a}_1+n_2\boldsymbol{a}_2)/a$$

where $|\boldsymbol{a}_1|=|\boldsymbol{a}_2|=a$, and $|\boldsymbol{a}_1\times\boldsymbol{a}_2|=a^2\sin 60^\circ$, n_1 and n_2 being integers (lattice vector). In the reciprocal lattice, the momentum component $\boldsymbol{q}_\perp$, perpendicular to the quantum wire axes, is defined as

$$\boldsymbol{q}_\perp=q_1\boldsymbol{b}_1+q_2\boldsymbol{b}_2$$

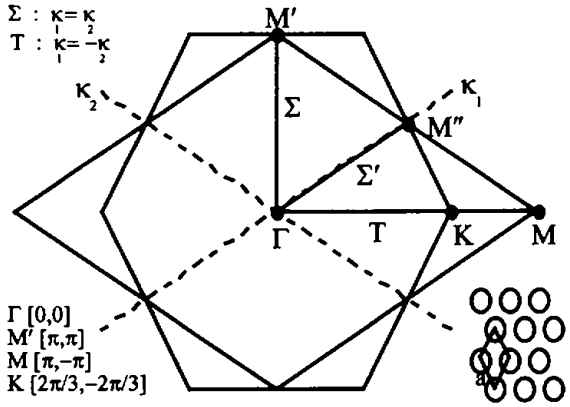

Figure 1. The three-dimensional quantum wire superlattice, seen in cross section, appears as a triangular close-packed Bravais lattice (lower right part of the figure). This figure depicts the primitive cell in the reciprocal two-dimensional lattice which may be considered a rhombus (with respect to the axes κ_1 and κ_2), or a hexagonal Brillouin zone. The plasmon frequency ω_p has been calculated for momentum κ ranging along two symmetry directions: (i) direction T, defined by $\kappa \equiv \kappa_1 = \kappa_2$, with the symmetry points $\Gamma[\kappa = 0]$, and $M'[\kappa = \pi]$; (ii) direction Σ, defined by $\kappa \equiv \kappa_1 = \kappa_2$, with the symmetry points $\Gamma[\kappa = 0]$, $K[\kappa = 2\pi/3]$ and $M[\kappa = \pi]$.

with $b_1 = a_2 \times u/|a_1 \times a_2|$ and $b_2 = u \times a_1/|a_1 \times a_2|$, u being the unit vector along the quantum wire axes; hence $a_i b_j = \delta_{ij}$.

In (2), e is the electron charge and $\Pi_1(q, \omega) = -\rho_1 q^2/m\omega^2$ is the one-dimensional electron polarization propagator where $\rho_1 = 2k_F/\pi$ is the density of electrons on the one-dimensional quantum wire. Equation (2) is obtained by noting that the longitudinal part of the Coulomb interaction between an electron located on a quantum wire, and another electron located at a distance r from the axis of that quantum wire, is given by

$$v_0(q, r) = 4\pi e^2 r_0 I_0(qr_0) K_0(qr) \qquad \text{with } r \geqslant 0 \tag{4}$$

r_0 being the radius of a quantum wire. In this equation I_0 and K_0 are the modified Bessel functions of the first and second kind, respectively. Because r_0 is small, $I_0(qr_0)$ can be replaced by 1. Moreover, since only the linear electron density is important, one-dimensional expressions like $\rho_1 = 2\pi r_0 \rho_2$ and $\Pi_1(q, \omega) = 2\pi r_0 \Pi_2(q, \omega)$ are introduced (a factor $2\pi r_0$ is removed from the potential and re-introduced into the propagator $\Pi_1 = 2\pi r_0 \Pi_2$). As a last step, $v_0(q)$ is introduced into (2) in the form

$$v_0(q) = 2e^2 K_0(q r_{nn'}) \tag{5}$$

where $r_{nn'}$ represents the distance between the axes of quantum wires n and n'. However, for electrons located on the same quantum wire ($n = n'$), K_0 is divergent, and the original argument qr_0 has to be kept in the term $\Delta n = 0$ of (3). Hence (3) is finally written as

$$F(q, \kappa) = K_0(qr_0) + \left[\sum_{n_1=-\infty}^{\infty} \sum_{n_2=-\infty}^{\infty} \mathrm{e}^{\mathrm{i}(\kappa_1 n_1 + \kappa_2 n_2)} K_0(qa|n|) - K_0(0) \right]. \tag{6}$$

The first term is a one-quantum-wire term. The second term (in brackets) includes the contribution of the other quantum wires distributed uniformly on a hexagonal lattice. The effective plasmon frequency for this 3DSL, $\omega_{p,\mathrm{eff}(q,\kappa)}$, is obtained by substituting (6) into (2).

For the sake of comparison, let us write down expressions for the plasmon frequencies of a single quantum wire and of a uniform 3DEG.

(i) A *one-quantum-wire* expression for $F(q,\kappa)$ is

$$F_{1qw}(q,\kappa) = K_0(qr_0)$$

where the subscript $1qw$ stands for one quantum wire. Substitution of this into (2) gives the plasmon frequency for a single quantum wire as

$$[\omega_{p,1qw}(q)]^2 = (2e^2\rho_1/m)q^2K_0(qr_0).$$

A similar formula has previously been derived for the plasmon frequency of a single carbon nanotube by the present authors [31].

(ii) A *uniform bulk* expression for $F(q,\kappa)$

$$F_{\text{uni3}}(q,\kappa) = (4\pi/\sqrt{3a^2})/(q^2+q_\perp^2) = \pi/aQ^2$$

with

$$q_\perp^2 = (4/3a^2)(\kappa_1^2+\kappa_2^2-\kappa_1\kappa_2)$$

gives

$$[\omega_{p,\text{uni3}}(q,\theta)]^2 = (4\pi e^2\rho_3/m)q^2/Q^2.$$

Note that a three-dimensional density $\rho_3 = \rho_1/(a^2\sin 60^\circ)$ has been introduced in this latter expression and that $q = Q\cos\theta$, θ being the angle between the wavevector Q and the quantum wire axis. $\omega_{p,\text{uni3}}(q,\theta)$ given by the above expression is the plasmon frequency of an isotropic bulk material, except that we have broken up the wavevector Q into two components q and $q_\perp$ ($q_\perp$ being perpendicular to the wire axis), for an easy comparison with the results of a single quantum wire or of an array of quantum wires.

In all our numerical calculations we have chosen the following data: we consider quantum wires with an electron density $\rho_s = 0.38$ Å^{-2} and a radius $r_0 = 3.39$ Å. This yields $\rho_1 = 2\pi r_0\rho_s = 8.13$ Å^{-1} for the linear density along the quantum wires. Moreover we choose $a = 3r_0 = 10.17$ Å for the inter-quantum-wire separation (distance between two adjacent quantum wires).

The plasmon frequencies have been calculated for momentum κ ranging along two symmetry directions: (i) direction T, defined by $\kappa \equiv \kappa_1 = -\kappa_2$, with the symmetry points $\Gamma[\kappa = 0]$, and $M'[\kappa = \pi]$; (ii) direction Σ, defined by $\kappa \equiv \kappa_1 = \kappa_2$, with the symmetry points $\Gamma[\kappa = 0]$, $K[\kappa = 2\pi/3]$ and $M[\kappa = \pi]$. This geometry is depicted in figure 1.

The plasmon frequencies $\omega_{p,\text{eff}}(q,\kappa)$, $\omega_{p,\text{uni3}}$ and $\omega_{p,1qw}$ are plotted in figures 2 and 3. In figure 2 we have plotted these plasmon frequencies as a function of the momentum component q parallel to the quantum wire axes. The solid curves and the dashed curves represent $\omega_{p,\text{eff}}$ and $\omega_{p,\text{uni3}}$, respectively, for seven values of κ (the momentum component perpendicular to the quantum wires), taken along the line $T \equiv \Gamma KM$ (see figure 1). These curves, labelled a, b, ..., g, correspond to $6\kappa/\pi = 0, 1, 2, \ldots, 6$, respectively. The two curves, a, related to $\kappa = 0$ (point Γ of figure 1), tend to the classical bulk plasmon frequency for $q \sim 0$. For all seven values of k, as aq increases, $\omega_{p,\text{eff}}$ moves toward the dotted curve corresponding to a single-quantum-wire result. This shift is significant even for relatively moderate values of aq ($\geqslant 1$) for curves e, f and g as indicated by the vertical lines. From this trend we could conclude that $\omega_{p,\text{eff}}$ will tend to $\omega_{p,1qw}$ for really large values of $aq(\gg 1)$. For small $aq(\approx 0)$, $\omega_{p,\text{eff}}$ approaches values of $\omega_{p,\text{uni3}}$ given by the dashed curves. This is clearly visible for curves a–d, but becomes obscure for curves e–g because of their close proximity at these values of aq. In the intermediate-wavelength range ($0 \ll aq \ll \infty$), however, $\omega_{p,\text{eff}}$ is significantly different from these two limits indicating a large contribution of the lattice.

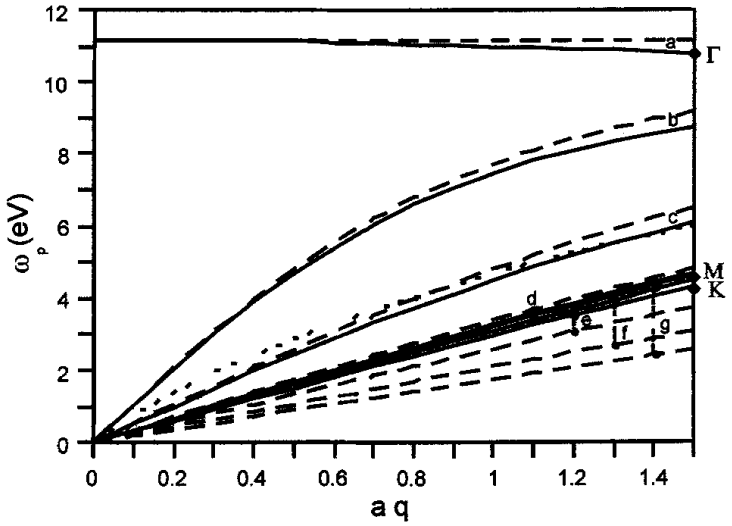

Figure 2. The effective plasmon frequency $\omega_{p,\mathrm{eff}}$ (solid curves) of the 3DSL along with $\omega_{p,\mathrm{uni3}}$ (dashed curves) are plotted as a function of q for seven values of κ. The curves labelled a, b, ..., g correspond to $6\kappa/\pi = 0, 1, 2, \ldots, 6$, respectively. The dotted curve gives the single-quantum-wire plasmon frequency $\omega_{p,1qw}$ (independent of κ).

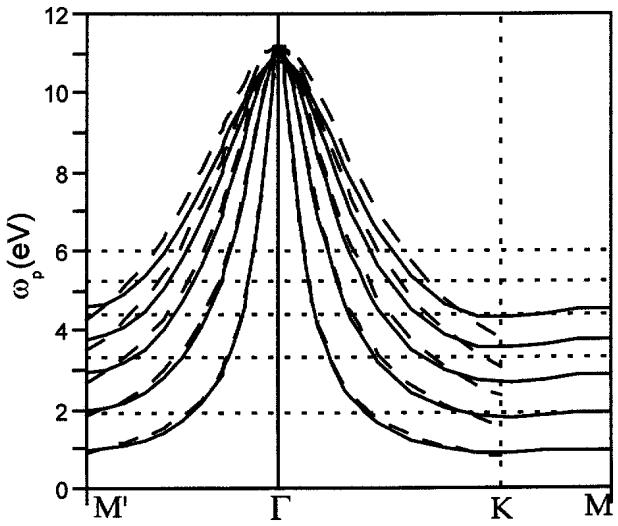

Figure 3. The plasmon frequencies $\omega_{p,\mathrm{eff}}$ (solid curves) and $\omega_{p,\mathrm{uni3}}$ (dashed curves) are plotted as a function of momentum κ for the two symmetry directions $\Sigma \equiv \Gamma M$ and $T \equiv \Gamma KM$ (see figure 1) for five values q (from top to bottom, $aq = 1.5$, 1.2, 0.9, 0.6 and 0.3). The horizontal dotted lines represent the plasmon frequency $\omega_{p,1qw}$ of a single quantum wire.

In figure 3 we plot the plasmon frequencies as a function of momentum κ (perpendicular to the quantum wires) for the two symmetry directions $\Sigma \equiv \Gamma M'$ and $T \equiv \Gamma KM$ (see figure 1). The solid curves and the dashed curves correspond to $\omega_{p,\mathrm{eff}}$ and $\omega_{p,\mathrm{uni3}}$, respectively, and the horizontal dotted lines to $\omega_{p,1qw}$, for five values of q (from top to bottom, one has

$aq = 1.5$, 1.2, 0.9, 0.6 and 0.3). For $q \sim 0$, these sets of curves coincide with the figure axes. Note that the right part beyond the K point of the figure (along $\Gamma K M$) presents the same features as figure 2. Obviously the plasmon dispersion is strong for momentum components both parallel and perpendicular to the quantum wires.

3. Conclusions

We have calculated the lowest subband collective electronic excitation modes (plasmon dispersion) of a quantum wire superlattice arranged in a hexagonal close-packed structure similar to the quantum wires in mesoporous silica (MCM-41). These effective plasmon frequencies along with those of a single quantum wire and of a 3DEG have been plotted in figures 2 and 3. It is seen in figure 2 that the direction along the axes of the quantum wires is the 'easy direction' for the excitations of the plasmons and thus for any q, the maximum occurs at the Γ-point. The plasmon frequency falls off when the effective wavevector deviates from the easy direction as seen in figure 3. The plasmon frequency has an acoustic behaviour at small q for all values of $\kappa \neq 0$ (figure 2). Figure 2 also shows that the 3DSL plasmon frequency begins to move toward that of a single quantum wire when the wavelength is comparable to or somewhat smaller than the inter-quantum-wire distance a ($aq \geqslant 1$), indicating that it would converge to $\omega_{p,1qw}$ for $aq \gg 1$. This figure also shows that the 3DSL plasmon frequency converges to the plasmon frequency of the uniform electron gas when the wavelength is large compared with a ($aq \ll 1$). The lattice contribution to the plasmon frequency is most significant at the intermediate wavelengths ($0 \ll aq \ll \infty$). Also, the plasmon dispersion is large for momentum components both parallel and perpendicular to the axes of the quantum wires.

The plasmon frequencies as calculated in this paper should be observable in the electron energy loss spectra (EELS), photoemission spectra, resonant inelastic light scattering (Raman spectra) etc of a quantum wire superlattice. The dispersion of the plasmon frequencies for momentum components parallel and perpendicular to the quantum wire axes has already been observed in a lateral distribution of quantum wires by Egeler *et al* [14]. More experiments are needed in 3DSLs of quantum wires as formed in MCM-41 to observe the nature of their plasmon frequencies.

References

[1] Notzel R and Ploog K H 2001 *Physica* E **8** 117
[2] Caalderman S *et al* 2000 *Phys. Rev.* B **62** 9935
[3] Wang X L *et al* 1997 *Superlatt. Microstruct.* **22** 221
[4] Panepucci R *et al* 1996 *Superlatt. Microstruct.* **20** 111
[5] Panepucci R *et al* 1995 *J. Vac. Sci. Technol.* B **13** 2752
[6] Iis P *et al* 1993 *J. Vac. Sci. Technol.* B **11** 2584
[7] Notomi M *et al* 1991 *Appl. Phys. Lett.* **58** 720
[8] Chen L *et al* 2001 *Physica* E **10** 368
[9] Volodin V A *et al* 1999 *Superlatt. Microstruct.* **26** 11
[10] Tkach M V *et al* 1999 *Condens. Matter Phys.* **2** 553
[11] Gold A 1994 *Z. Phys.* B **94** 395
[12] Schmeller A *et al* 1994 *Phys. Rev.* B **49** 14 778
[13] Li Q P and Das Sarma S 1991 *Phys. Rev.* B **43** 11 768
[14] Egeler T *et al* 1990 *Phys. Rev. Lett.* **65** 2704
[15] Romanov S G *et al* 1997 *J. Appl. Phys.* **82** 380
[16] Tonucci R J *et al* 1992 *Science* **258** 783
[17] Skelton E F *et al* 1991 *Science* **253** 1123

[18] Kresge C T *et al* 1992 *Nature* **359** 710
[19] Huo Q *et al* 1994 *Nature* **368** 317
[20] Hirai T *et al* 1999 *J. Chem. Phys.* B **103** 4228
[21] Parala H *et al* 2000 *Adv. Mater.* **12** 1050
[22] Srdanov V I *et al* 1998 *J. Chem. Phys.* B **102** 3341
[23] Aggar J R *et al* 1998 *J. Chem. Phys.* B **102** 3345
[24] Leon R *et al* 1995 *Phys. Rev.* B **52** R2285
[25] Tang Y S *et al* 1997 *Appl. Phys. Lett.* **71** 2449
[26] Chen L *et al* 2001 *Physica* E **10** 368
[27] Bose S M and Longe P 1992 *J. Phys.: Condens. Matter* **4** 1799
[28] Luttinger J M 1963 *J. Math. Phys.* **4** 1154
[29] Jerome D and Schulz H J 1962 *Adv. Phys.* **31** 299
[30] Schulz H J 1983 *J. Phys. C: Solid State Phys.* **16** 6769
[31] Longe P and Bose S M 1993 *Phys. Rev.* B **48** 18 239